

RESEARCH
ARTICLE

Zero-Point Energy: Capturing Evanescence

Garret Model

Department of Electrical,
Computer, and Energy Engineering

Radanta Corporation
Boulder, Colorado, USA

SUBMITTED April 6, 2021
ACCEPTED June 29, 2022
PUBLISHED October 22, 2022

<https://doi.org/10.31275/20222567>

PLATINUM OPEN ACCESS



Creative Commons License
4.0. CC-BY-NC. Attribution
required. No Commercial use.

HIGHLIGHTS

Combining quantum vacuum and nanoelectronic device concepts results in a novel energy-producing device that seemingly draws energy from the quantum vacuum.

ABSTRACT

In results from thousands of trials and dozens of variations, tests for measurement artifacts, and replications, metal/insulator/metal/Casimir cavity devices produce electric power, apparently by tapping ambient zero-point energy (ZPE). A simple calculation shows that the power potentially available from the ZPE quantum vacuum is an immense 5 gigawatts per square meter. The devices tap a tiny fraction of that, but still deliver a practical power density of 70 watts per square meter. The devices are designed to circumvent the apparent impediments to ZPE harvesting, i.e., that ZPE is the universal ground state, and that ZPE fluctuations are extremely short-lived and virtual. If the source ultimately proves to be ZPE, what is the operating principle behind the energy harvesting, and how can the results be reconciled with known physical law? A notional operating principle can be understood as a direct analog to the optical phenomenon of frustrated total internal reflection. Tapping ZPE does not violate the second law of thermodynamics based on the conventional quantum interpretation of ZPE, but ambiguities regarding the source of ZPE leave the issue unresolved.

INTRODUCTION

The concept of expending resources to obtain energy has remained with us for most of human history, with the mining of carbon-based fuels, reacting of nuclear fuels, and collecting of sunlight, etc., to provide energy. From that perspective, the harvesting of zero-point energy (ZPE), a still mysterious cache of ubiquitous energy, feels like a violation of the principles of the world as we have come to know it. Can we tap this energy, or would doing so violate fundamental principles?

It appears that our lab has, in fact, discovered and demonstrated a way to tap ZPE (Model et al. 2021a; Model, 2021c). In this article, I review how we have done this and describe the underlying issues. First comes ZPE basics, including for the first time how much power can be

obtained from the quantum vacuum ZPE. This is followed by the technology we have developed to harvest it, and the results. Then, I examine the impediments to harvesting ZPE fluctuations, including a way to understand the extraction of energy from what are termed virtual particles. This article addresses whether harvesting ZPE would violate the second law of thermodynamics, and where the energy might ultimately be coming from. The appendices comprise the equations and calculations on the available power, and a description of the sanity checks that were carried out to investigate whether the results could be due to unaccounted for artifacts. We are still in the midst of discovery and this article represents our current understanding, which is certain to evolve over time.



ZERO-POINT ENERGY BACKGROUND INFORMATION

ZPE is the ground state energy of quantum mechanical systems in both empty space and matter. In empty space it results in electromagnetic field fluctuations (Milonni, 2013). In molecules and solids it excites vibrations (quantized as phonons) (Yang & Kawazoe, 2012). With the further addition of conducting carriers (such as electrons) it results in plasmonic fluctuations (collective charge oscillations) (Rivera et al., 2019).

In 1900, Max Planck developed his revolutionary theory for blackbody radiation that fills space. This thermal blackbody radiation for room temperature (300 K) is shown in Figure 1 as the curve that cups downward. It peaks at a photon energy of roughly 0.1 eV, corresponding to an infrared wavelength of 12 μm , and falls off before reaching the visible spectrum.

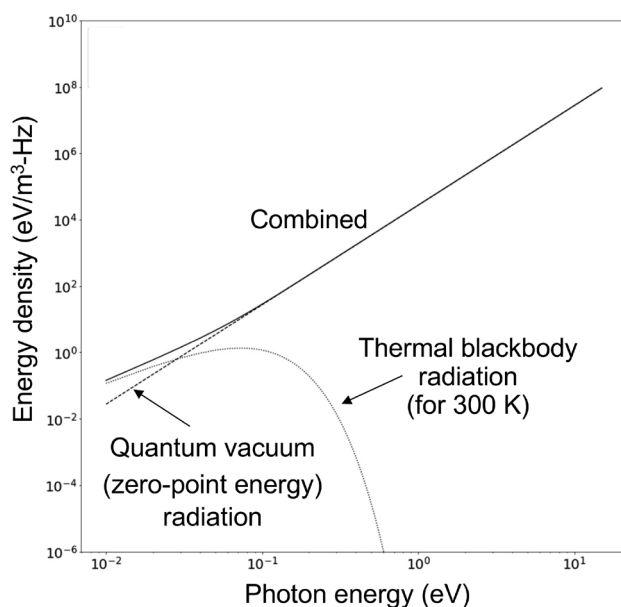


Figure 1. Energy density of background electromagnetic fields at room temperature ($T = 300\text{ K}$), as a function of photon energy (plot by Matt McConnell).

Eleven years after presenting his first theory Planck presented his second theory, which contained an additional, temperature-independent term. The full expression for the energy density of both the thermal blackbody, at temperature T , and ZPE components is

$$\rho(hf) = \frac{8\pi f^2}{c^3} \left(\frac{hf}{\exp(hv/kT) - 1} + \frac{hf}{2} \right) \quad (1)$$

where h is Planck's constant, f is the frequency of the radiation, and c is the speed of light (Milonni, 2013).

Planck called the latter component, shown as the second term on the righthand side of the equation, *Restenergie* (rest energy) (Kragh 2012). Two years later, Albert Einstein and Otto Stern termed it *Nullpunktenergie* (ZPE), because it exists even at a temperature of zero. In 1916, Nernst characterized ZPE as filling not only space (which he called the ether) but also material objects. At the time, Planck's second theory and the notion of ZPE was rejected by the physics community and only became increasingly accepted starting in 1926, when the uncertainty principle in the then-evolving quantum mechanics required it. The energy density for ZPE is shown as the straight line in Figure 1. At photon energies above those of mid-infrared light, the ZPE part of the energy spectrum dominates.

Usually, the energy density of ZPE is given, but that is not directly relevant to energy harvesting. For harvesting, it is the flow of energy, i.e., the power and the current, that matter. I derive the mathematical expression for those quantities in Appendix I, and find the cumulative magnitude up to a given (cutoff) photon energy. The cumulative current density grows with the third power of the cutoff photon energy (hf) and the power density with the fourth power of cutoff photon energy. The radiation passing through a given area can be expressed in terms of photon current, which is defined as the electrical current that would be produced if each incident photon generated the current from one electron. The ZPE cumulative photon current is shown in Figure 2.

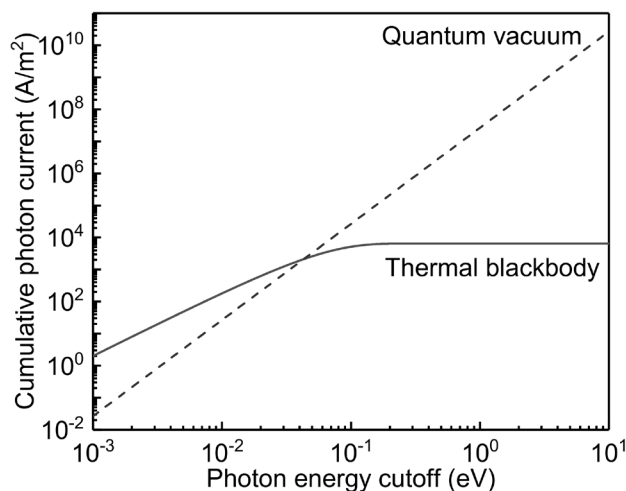


Figure 2. Cumulative photon current up to a cutoff photon energy from background electromagnetic radiation at room temperature, showing the thermal blackbody and quantum vacuum (zero-point energy) components. Photon current is defined as the electrical current that would be produced for each incident photon generating the current from one electron. The derivation of the expression for these currents is given in Appendix I.

The cumulative photon currents from the ZPE spectrum are huge. For example, the current produced for a cut-off photon energy of 4 eV, corresponding to a wavelength of 0.3 μm , is 1.7 GA m^{-2} , i.e., more than one billion amps per square meter. For comparison, a solar cell produces roughly 350 A m^{-2} .

The power available from the quantum vacuum for the same cutoff photon energy of 4 eV, as calculated in Appendix I, is 5.0 GW m^{-2} . For comparison, an entire full-size coal-fired power plant generates about 5 GW, the same amount of ZPE that passes through just one square meter. As described below, the power density that we have obtained so far is much lower than what is available, but even so it is sufficient to provide practical power levels.

DEVICE DESCRIPTION AND RESULTS

Device Structure

A depiction of the cross section of one of the devices being fabricated in our laboratory is shown in Figure 3(a). The device consists of an optical cavity deposited on top of a metal-insulator-metal (MIM) diode. The optical cavity, also called a Casimir cavity as discussed later in this article, consists of two reflective layers surrounding a transparent dielectric medium, either a polymer, polymethyl methacrylate (PMMA), or an oxide, SiO_2 . The cavity thickness ranges from 33 nm to 1100 nm. The MIM diode consists of a semi-transparent palladium layer, 8.3 nm thick, and a thicker nickel layer surrounding a very thin insulator, ~2 nm in thickness. The insulator is thin enough for charge carriers to tunnel through it.

The devices are formed using microfabrication techniques described in Model et. al. (2021a). Although devices

have been produced with a wide range of areas, those with submicron areas have produced the highest power density thus far. A scanning electron microscope image of one of the devices is shown in Figure 3(b). Its active region, formed at the overlap of palladium and nickel regions with a thin insulator in between, has an area of 0.02 μm^2 . An optical Casimir cavity is formed over the MIM structure.

Results

The presence of an adjoining optical cavity results in a radical change in the current-voltage $I(V)$ characteristics of the MIM diode. Its resistance is greatly reduced (Model, 2021b), but more significantly, it produces power. The $I(V)$ curve for a device with a 33 nm thick transparent dielectric is shown in Figure 4(a). If an $I(V)$ curve does not pass through the origin it either uses or produces power ($I \times V$), with the second and fourth quadrants of the $I(V)$ graph corresponding to power production.

The fact that the device produces power in the absence of any apparent input is remarkable. The area and $I(V)$ characteristics for the device shown correspond to a power production of 70 W/ m^2 . This is roughly one-third of the power per unit area produced by solar cells. Because this device is not optimized and can, in principle, be stacked, if the concept scales as it appears to, very substantial and practical power levels can be expected in the future.

As will be discussed later in this article, a signature of ZPE is an increasing deficit in energy density as the thickness of an optical cavity is reduced. The data of Figure 4(b) show just such a trend, with increasing power produced by devices for thinner cavities that are filled with PMMA or with SiO_2 .

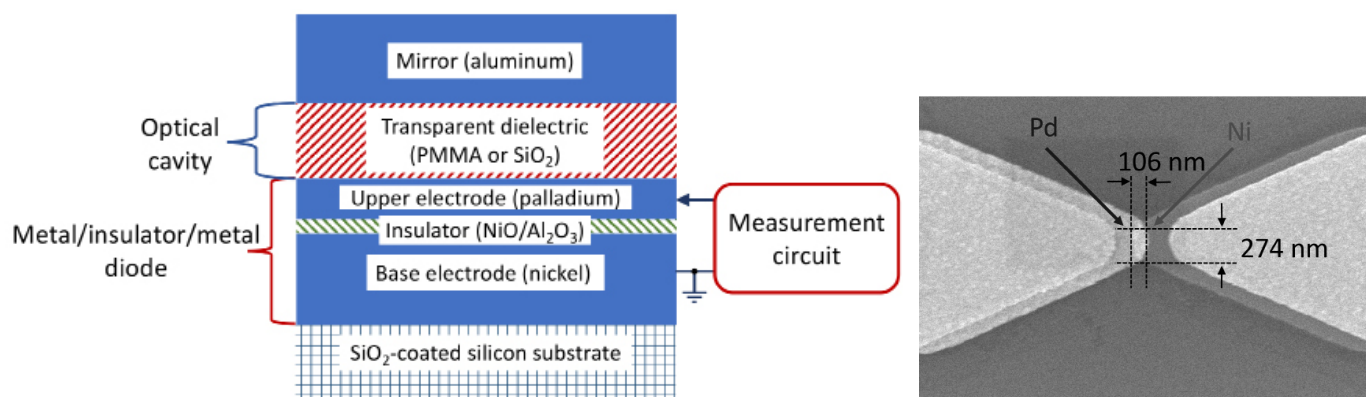


Figure 3. (a) Device cross-section, showing a metal-insulator-metal (MIM) structure adjoining an optical cavity. Positive current is defined to be in the direction of the arrow. **(b)** A scanning electron microscope (SEM) image of the top view of a completed MIM device. Both images are from Model (2021a).

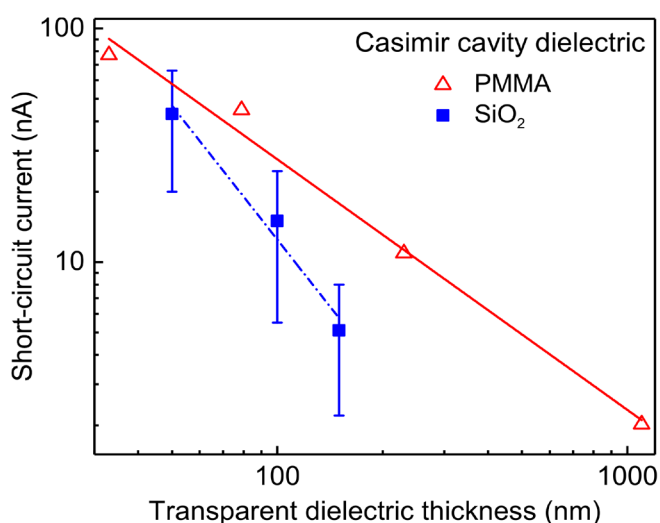
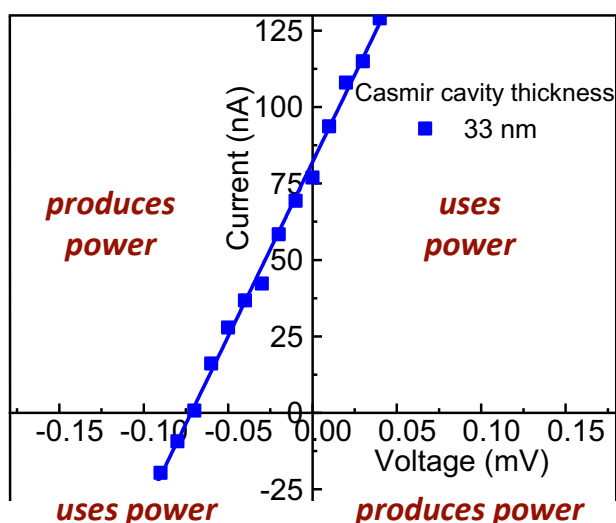


Figure 4. (a) Current as function of voltage for a device having a 33 nm cavity filled with PMMA. The curve passes through the second quadrant of the graph, corresponding to power production. The power density is 70 W/m². **(b)** Short-circuit current as a function of cavity thickness for PMMA and SiO₂-filled cavities (from Modde, 2021a). The output decreases with increasing thickness of the cavity, a signature of ZPE.

Testing for Artifacts

The trends shown here have been replicated in many thousands of devices produced in dozens of batches, although with significant device-to-device variation due to poorly controlled fabrication parameters in our current fabrication process. To analyze whether the devices are genuinely producing power, we carried out an in-depth investigation of nine possible artifacts (Model 2021a). The main points are summarized in Appendix II. No possible artifact that we are aware of can explain the observed results.

IMPEDIMENTS TO HARVESTING ZERO-POINT ENERGY

Universal Ground State

ZPE is the universal ground state, and it stands to reason that without a gradient (slope) or step in the ZPE density no flow can be induced. A change in this ground state can, however, be induced because it is geometry-dependent. In 1948, Hendrik Casimir proposed that the ZPE density in between two closely spaced mirrors would be lower than outside (Casimir, 1948). In particular, only zero-point electromagnetic modes having wavelengths of twice the optical cavity spacing divided by an integer are supported in this Casimir cavity, and all wavelengths greater than twice the spacing are suppressed. The reduction in mode density is depicted in Figure 5. As will be discussed,

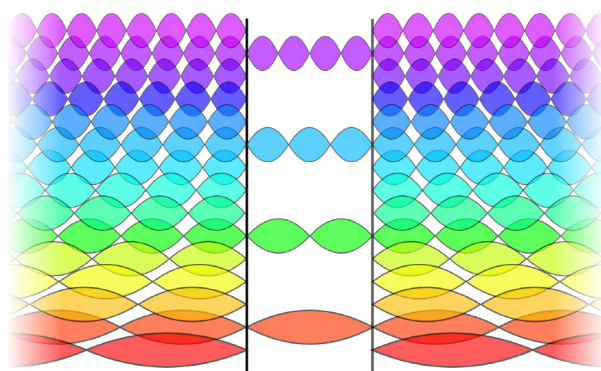


Figure 5. Depiction of optical modes in a Casimir cavity, where only limited wavelengths are allowed and long wavelength zero-point electromagnetic modes are suppressed (image from Kingsbury [2009]).

our devices make use of an adjoining optical cavity to provide a step in the ZPE density.

Short-Lived Fluctuations

The Heisenberg uncertainty principle limits the accuracy with which the values of certain complementary pairs of physical quantities are meaningful. One such pair is the energy and time, so that the lower the uncertainty is in the energy (ΔE) of a particle the greater the uncertainty must be in the time (Δt) that it is observable. In a vacuum, this means that large energy ZPE fluctuations can exist for only

short times. For example, fluctuations having a photon energy of 2 eV (corresponding to red light), can exist for a time of only 0.16 fs (one femtosecond is 0.000000000000001 seconds). A theory has been proposed that an energy ΔE may be borrowed from the vacuum for a time Δt as long as it is paid back (Ford, 1991; Davies & Ottewill, 2002; Huang & Ford, 2015). The question I pondered is what would happen if the energy of the fluctuation were captured extremely quickly and in such a way that it could not be returned. As discussed in the Device Concept section, our devices make use of femtosecond capture of transitory energized particles.

Virtual Particles

When sufficiently energetic electromagnetic radiation strikes a metal surface, electrons are emitted, as depicted in Figure 6. This photoelectric effect was observed by Heinrich Hertz in 1887 and explained in terms of photon energy in 1905 by Einstein.

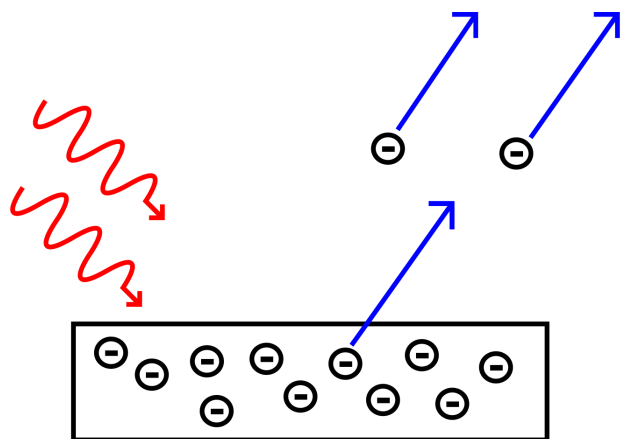


Figure 6. The photoelectric effect, in which incident electromagnetic radiation onto a metal surface produces the emission of electrons. (Image from Wikimedia Commons, https://commons.wikimedia.org/wiki/File:Photoelectric_effect.svg)

Given the ubiquitous zero-point background electromagnetic fields shown in Figure 1, the question arises as to why we do not observe emission of electrons from all metal surfaces as a result of these fields. We can address this issue in terms of the short-lived nature of the fluctuations described in the previous section. For the example of 2 eV radiation (red light) presented above, the Δt is 0.16 fs. A simple calculation shows that in that time an electron would travel only 1 Å (0.1 nm), roughly an interatomic dis-

tance, before the borrowed fluctuation energy would be returned.

Another perspective on short-lived fluctuations is via the concept of virtual particles. Although the distinction between real and virtual particles is debated (Jaeger, 2019), ZPE quantum vacuum electromagnetic waves are generally considered to be virtual. Virtual waves and particles are transient quantum fluctuations whose existence is limited by the uncertainty principle, and which mediate interactions between other particles. Because they can be observed only through their effect on other particles, one cannot capture a “naked” virtual particle. They can, however, be converted to real particles. In the dynamical Casimir effect, effectively moving the mirrors of a Casimir cavity at high velocity has been shown to convert virtual fluctuations into real photons (Wilson et al., 2011). Can ultra-fast capture also convert virtual particles to real ones? By way of a comparison with evanescent optical modes, I argue that the answer may be yes.

Evanescent waves are oscillating electromagnetic waves that do not propagate; they just stay in one place. Such evanescent waves are equivalent to virtual photons (Stahlhofen, 2006). An evanescent wave is formed at the interface where total internal reflection occurs. Total internal reflection is an optical phenomenon that occurs in a prism where light is incident at an angle greater than a critical angle, as depicted in Figure 7(a). The evanescent wave extends beyond the prism and falls off exponentially within a fraction of wavelength. If a second prism is placed more than a wavelength away from the first, as shown in Figure 7(b), the evanescent wave is not affected. If, however, the second prism is placed within a small fraction of

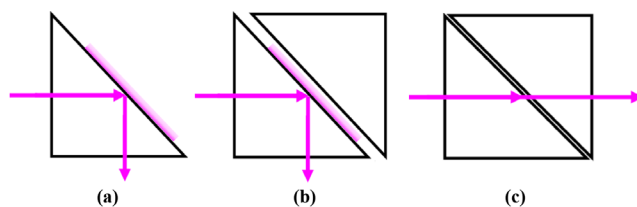


Figure 7. Converting evanescent waves into propagating waves. (a) Total internal reflection inside a prism, with an evanescent wave extending beyond the prism. (b) Second prism placed several wavelengths away from first prism does not affect the evanescent wave. (c) Second prism placed within a small fraction of a wavelength away from first prism frustrates the total internal reflection, resulting in a propagating wave. A side note: the evanescent coupling distance is limited by the same $\Delta E \Delta t$ uncertainty relation that controls zero-point fluctuations (Model, unpublished).

a wavelength from the first prism, evanescent coupling occurs; the previously stationary wave becomes a propagating wave, as depicted in Figure 7(c). In this way, the total internal reflection is frustrated (Hecht, 2017). The evanescent wave is turned into a propagating wave by the proximity of a second prism, a visible example of quantum tunneling through the narrow gap.

The same process is followed in our devices, in which an evanescent wave at a barrier becomes a propagating wave when the barrier region is sufficiently thin. This is depicted in Figure 8, where the incident wave is composed of electrons in a metal layer (such as the upper electrode in our device). The barrier is an insulator, and when that insulator layer is sufficiently thin some of the electron wave tunnels through and is transmitted to the second metal layer (the base electrode in our device). The energetic electrons are rapidly captured in the second metal layer. As described in the next section, this electron transport is the second step in a virtual particle chain.

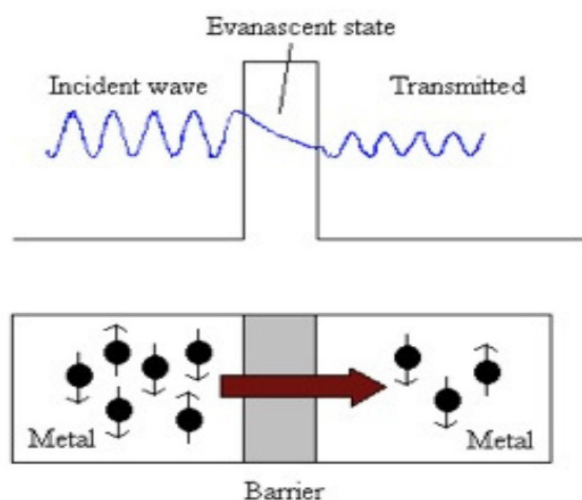


Figure 8. Evanescent coupling in a metal–insulator–metal device. The insulator forms a barrier through which the electron wave quantum mechanically tunnels, which is equivalent to evanescent coupling. Quantum tunneling is constrained by same $\Delta E \Delta t$ uncertainty relation that constrains zero-point fluctuations (Fertig, 1990). (Figure reproduced from Bhansali et al., 2010).

DEVICE CONCEPT

The device concept to harvest ZPE was developed five years ago, submitted as a provisional patent application three years ago, and the patent was issued recently (Model, 2021c). Subsequent experimental results have shown that an effective structure and the output characteristics

of the device, depicted in Figures 3 and 4, closely follow what was predicted. As described below, it appears that the device works as a result of an asymmetry induced by the presence of an adjoining Casimir cavity. At this point, that model for the device operation is still speculative, and it is possible that the device structure has fortuitously enabled energy harvesting by a different mechanism. Here, I describe the apparent operating concept.

The ZPE harvesting device is based on MIM diodes, devices which our lab has been designing and fabricating for more than two decades to provide ultrahigh speed rectification (Grover & Model, 2012). These devices work by incorporating an ultra-thin barrier that allows charge carriers, electrons or holes, to tunnel through, as depicted in Figure 8. (Although the term “diode” usually refers to devices that allow current to flow preferentially in one direction, the MIM diodes do not necessarily exhibit asymmetry in current flow.) Tunneling through, or excitation over, the 1 to 3 nm thick insulator occurs in roughly 1 fs. The ZPE harvesting devices incorporate MIM diodes that have a base layer that is sufficiently thick (>35 nm) to be opaque, and a thinner (~10 nm) semitransparent upper electrode.

The photoelectric effect, depicted in Figure 6, produces emission of electrons at the free surface. If the metal layer is sufficiently thin, then the excited electrons also produce internal photoemission (also called photoinjection) at the internal surface. An MIM diode having a semitransparent upper electrode is depicted in Figure 9(a). At the upper surface, incoming zero-point radiation excites hot charge carriers that contribute to downward flow of charges. In addition, internal ZPE fluctuations in the upper electrode excite charges that contribute to that downward flow. The combined photoinjection and internally excited charges result in the downward flow depicted by the arrow on the left. The actual current that is produced is subject to the same constraints that block any ZPE-excited current in the photoelectric configuration shown in Figure 6. I term this loosely as a virtual current.

Similarly, internal ZPE fluctuations in the base electrode excite charges that result in an upward flow. There is no photoinjection current contributing to the upward charge flow because the base electrode is too thick for photoexcited charge generated at the lower surface to traverse the electrode to the insulator before being scattered. Because the base electrode is thicker than the upper electrode it produces more internally generated charge, so that the total upward charge flow is equal to the downward flow.

Now consider the same MIM diode, but with an adjoining Casimir cavity over the upper electrode, as shown in Figure 9(b). As discussed with regard to Figure 5, the zero-point electromagnetic mode density in a Casimir cavity is

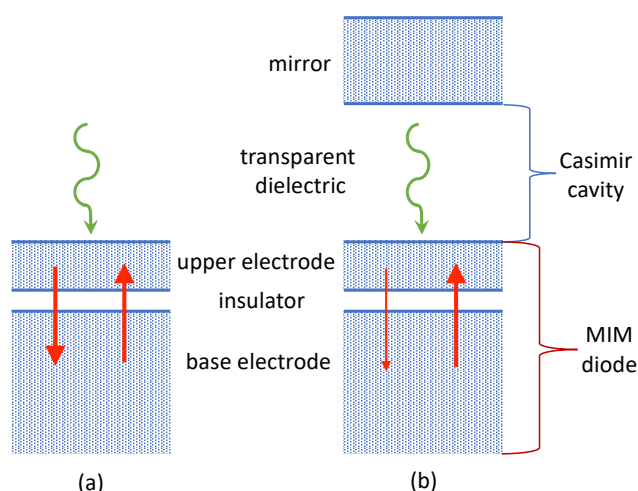


Figure 9. Device cross sections showing operating concept. **(a)** MIM diode with a thin upper electrode, which permits the photoinjection of charge from free space zero-point electromagnetic fluctuations. The downward flow of photoinjected charge plus internally excited charge is balanced by the upward flow of internally excited charge. **(b)** MIM diode with an adjoining Casimir cavity above the upper electrode, which results in suppression of photoinjection and reduces the downward flow of charge.

reduced as compared to the mode density in free space. Therefore, the photoinjection current is partially suppressed and the downward charge flow is reduced. Since the upward flow is not changed by the addition of the Casimir cavity, there is now a net flow of charge in the upward direction. This is a simplistic conceptual explanation for the current that we observe. The actual mechanisms are more complex and involve emission of electromagnetic modes into the cavity as well as absorption from the cavity, and are constrained by the transient nature of the zero-point excitations as required by the uncertainty principle, and can include contributions to the current from both electrons and holes.

I speculate on the chain of events that facilitates the capture of ZPE. Virtual photons strike the upper electrode and produce a virtual current of charge carriers that traverse the thin metal layer and the insulator, and are captured in the base electrode. Just as virtual photons that form an evanescent wave are converted to real, propagating photons in the presence of evanescent coupling, so too the virtual photons and subsequent virtual charge flow are converted into a real charge flow as a result of tunneling through the insulator and capture in the base electrode of our devices. As an alternative to invoking the notion of virtual particles, the $\Delta E \Delta t$ uncertainty relation limits the time available for the process to occur. If the transit and capture are completed within roughly 1 fs, then the energy may be

captured; if not, then the energy is returned. Even if the process is not completed within the 0.16 fs described in the section on Short-Lived Fluctuations, some fraction of the available current can be collected, including from lower energy and hence longer-lived excitations. The presence of the adjoining Casimir cavity upsets the balance in virtual charge flow that would exist with it, so that the net flow of charge is upward.

This operating model is notional at best, and is far from rigorous. In contrast, a rigorous quantum model (Ford, 2022) has been proposed to explain the increase in conductivity that we observe due to an adjoining Casimir cavity (Model, 2021b), but it does not explain the observed power production.

LAWS OF THERMODYNAMICS

The second law of thermodynamics describes limits on the amount of heat that can be converted into work, and the inability of heat at the same temperature as its surroundings to be converted to work. There are multiple versions of the second law (Čápek & Sheehan, 2005), most of which involve the concept of temperature. Because ZPE exists even in the absence of temperature, to analyze the possibility of harvesting ZPE requires a version of the second law that does not involve temperature. Planck's version of the second law states, "Every . . . process occurring in nature proceeds in such a way that the sum of the entropies of all bodies which participate . . . is increased." Since work (including electrical power) has zero entropy, converting an entropy-containing source of energy, such as heat, would violate the second law unless the excess entropy is carried away via heat loss. Entropy is a measure of the number of options for the configuration of energy in a system. ZPE in free space is a unique ground state, the only option, and therefore has zero entropy (Boyer, 2002). For that reason, we are free to convert ZPE in free space to work without violating the second law.

The situation is different in a Casimir cavity, where the entropy is not zero and is associated with the cavity spacing (Revzen et al., 1997). Therefore, if the cavity spacing is varied as the energy is extracted, e.g., making use of the Casimir force to produce work, there will be a change in the entropy of the system. To avoid the need to decrease the entropy of the system and violate Planck's version of the second law, heat would then have to be expelled to carry the entropy away. This would limit how much, if any, of the ZPE could be converted to work. In the ZPE harvesting system described here, however, there is no change in the cavity spacing, and therefore no change in the internal entropy. Therefore, we are free to convert the ZPE to work without necessarily violating the second law.

If ZPE is being extracted from quantum vacuum fluctuations, a crucial question is what is the nature of the underlying source for that energy:

- ZPE is built into quantum mechanics, which leads to the disconcerting notion that if one were to extract ZPE from a closed system, the amount of ZPE in that system would remain unchanged. Extracting ZPE would then violate conservation of energy, the first law of thermodynamics, even if it did not violate the second law.
- An alternative view of ZPE is described by stochastic electrodynamics (Boyer, 1975), an intriguing but incomplete classical alternative to quantum mechanics in which space is filled with real electromagnetic ZPE that is dynamically exchanged between matter and space. A stochastic electrodynamics model would allow for extraction of ZPE without violating the first or second laws of thermodynamics.
- Finally, I speculate about a “thermal model,” in which the source for ZPE is ultimately thermal. ZPE and thermal energy are intimately connected (Boyer, 2012), but the notion that there is an exchange of energy between these two entities is certainly not accepted. Despite that, if it were to turn out that draining the ZPE from a system ultimately tapped the thermal energy in the system, harvesting ZPE would then cool the system; that would violate multiple versions of the second law.

If our devices are in fact powered by ZPE, a study of the extraction process could help explain the ultimate source of that energy.

CONCLUSIONS

Are we somehow fooling ourselves? We have carried out many tests for artifacts and they have all come out negative (briefly described in Appendix II). Recently multiple labs that are known for measurement accuracy have tested our devices in highly controlled environments and reproduced what we measure (not yet published). We have observed consistent trends in dozens of different device runs and thousands of measurements.

What we observe is real, but what is it due to? I have a continuing debate with myself, and anyone else who pipes in, as to whether the energy production that we observe is from ZPE, or if there is there some other source. The power output requires an adjoining optical cavity, and varies inversely with the cavity thickness—consistent with a ZPE source. The output varies with insulator and upper electrode thickness in a way that is consistent with photo-injection. Recent observation has shown that the effect

does not diminish with decreasing temperature (not yet published)—also consistent with a ZPE source.

The quantum electrodynamics theory for the quantum vacuum and ZPE is rigorous, but still ambiguous as to the nature of ZPE. New characteristics of the Casimir effect are still be discovered. Given the evolving nature of our understanding of ZPE, must theory lead and experiment follow? Looking at the history of scientific advancement, I think not. “We don’t want to lose sight of the fundamental fact that the most important experimental results are precisely those that do *not* have a theoretical interpretation” (Anderson, 1990).

Why are there no other clear observations of ZPE harvesting despite various approaches that have been proposed (Model & Dmitriyeva, 2019)? Is it possible that my speculations are correct that the key is femtosecond capture of the energy, and our devices are (to the best of our knowledge) unique in their ability to extract and capture the energy so quickly?

This is a fascinating adventure. Even more significantly, if these devices are, in fact, harvesting ZPE, then the technology could be truly world-changing for a world that desperately needs a clean and relatively cheap power source. The devices we are currently fabricating are tiny, but device technology has repeatedly shown the capability of scaling up. If even a small fraction of the 5 GW/m² power that I calculated were available from the quantum vacuum, it would provide all the power that we need for the foreseeable future.

ACKNOWLEDGEMENTS

I gratefully acknowledge Ayendra Weerakkody, Dave Doroski, and Dylan Bartusiak, the team that designed, fabricated, and tested the devices described in Model (2021a), and more recent members of the team, Bradley Pelz and Kyuyoung Bae. I appreciate the comments on the manuscript provided by Matt McConnell and Swapnil Mhatre. Without the encouragement and support of Matt McConnell this endeavor would not have been possible. Much of the work was supported by The Denver Foundation, which I greatly appreciate, and more recently by Radanta Corporation.

REFERENCES

- Anderson, P. (1990). Solid-state experimentalists: Theory should be on tap, not on top. *Physics Today*, 43(9), 9–10. <https://physicstoday.scitation.org/doi/10.1063/1.2810678>
- Bhansali, S., Krishnan, S., Stefanakos, E., & Goswami, D. Y. (2010, December). Tunnel junction based rectenna—A key to ultrahigh efficiency solar/thermal energy

- conversion. In *AIP Conference Proceedings*, 1313(1), (pp. 79–83). American Institute of Physics. <https://aip.scitation.org/doi/pdf/10.1063/1.3530572>
- Boyer, T. H. (1975). Random electrodynamics: The theory of classical electrodynamics with classical electromagnetic zero-point radiation. *Physical Review D*, 11(4), 790. <https://journals.aps.org/prd/abstract/10.1103/PhysRevD.11.790>
- Boyer, T. H. (2002). Connecting blackbody radiation and zero-point radiation within classical physics: A new minimum principle and a status review. *arXiv preprint physics/0206033*. <https://arxiv.org/abs/physics/0206033>
- Boyer, T. H. (2012). The blackbody radiation spectrum follows from zero-point radiation and the structure of relativistic spacetime in classical physics. *Foundations of Physics*, 42(5), 595–614. <https://link.springer.com/content/pdf/10.1007/s10701-012-9628-x.pdf>
- Cápek, V., & Sheehan, D. P. (2005). *Challenges to the second law of thermodynamics* (pp. 202–203). Springer. <https://link.springer.com/article/10.1007/s10701-012-9628-x>
- Casimir, H. B. (1948). On the attraction between two perfectly conducting plates. In *Proceedings of the Koninklijke Nederlandse Akademie van Wetenschappen*, 51 (p. 793).
- Davies, P. C. W., & Ottewill, A. C. (2002). Detection of negative energy: 4-dimensional examples. *Physical Review D*, 65(10), 104014.
- Fertig, H. A. (1990). Traversal-time distribution and the uncertainty principle in quantum tunneling. *Physical review letters*, 65(19), 2321.
- Ford, L. H. (1991). Constraints on negative-energy fluxes. *Physical Review D*, 43(12), 3972.
- Ford, L. H. (2022). Electric field and voltage fluctuations in the Casimir effect. *Physical Review D*, 105(6), 065001.
- Grover, S., & Model, G. (2012). Engineering the current-voltage characteristics of metal-insulator-metal diodes using double-insulator tunnel barriers. *Solid-State Electronics*, 67(1), 94–99. <https://www.sciencedirect.com/science/article/abs/pii/S0038110111003224>
- Hecht, E. (2017). *Optics, Fifth Edition*. Pearson.
- Huang, H., & Ford, L. H. (2015). Quantum electric field fluctuations and potential scattering. *Physical Review D*, 91(12), 125005. DOI: 10.1103/PhysRevD.91.125005
- Jaeger, G. (2019). Are virtual particles less real? *Entropy*, 21(2), 141. <https://www.mdpi.com/1099-4300/21/2/141>
- Kingbury, K. (2009). The Casimir Effect. <https://aphyr.com/media/comps.pdf>
- Kragh, H. (2012). Preludes to dark energy: Zero-point energy and vacuum speculations. *Archive for History of Exact Sciences*, 66(3), 199–240. <https://link.springer.com/article/10.1007/s00407-011-0092-3>
- Milonni, P. W. (2013). *The quantum vacuum: An introduction to quantum electrodynamics*. Academic Press.
- Model, G., & Dmitriyeva, O. (2019). Extraction of Zero-Point Energy from the vacuum: Assessment of stochastic electrodynamics-based approach as compared to other methods. *Atoms*, 7(2), 51. <https://www.mdpi.com/2218-2004/7/2/51>
- Model, G., Weerakkody, A., Doroski, D., & Bartusiak, D. (2021a). Optical-cavity-induced current. *Symmetry*, 13(3), 517. <https://www.mdpi.com/2073-8994/13/3/517>
- Model, G., Weerakkody, A., Doroski, D., & Bartusiak, D. (2021b). Casimir-cavity-induced conductance changes. *Physical Review Research*, 3(2), L022007. <https://journals.aps.org/prresearch/abstract/10.1103/PhysRevResearch.3.L022007>
- Model, G. (2021c). U.S. Patent No. 11,133,758. Washington, DC: U.S. Patent and Trademark Office. <https://patents.google.com/patent/US11133758B2/en>
- Revzen, M., Opher, R., Opher, M., & Mann, A. (1997). Casimir's entropy. *Journal of Physics A: Mathematical and General*, 30(22), 7783.
- Rivera, N., Wong, L. J., Joannopoulos, J. D., Soljačić, M., & Kaminer, I. (2019). Light emission based on nanophotonic vacuum forces. *Nature Physics*, 15(12), 1284–1289. <https://www.nature.com/articles/s41567-019-0672-8>
- Stahlhofen, A. A., & Nimtz, G. (2006). Evanescent modes are virtual photons. *EPL (Europhysics Letters)*, 76(2), 189. <https://iopscience.iop.org/article/10.1209/epl/i2006-10271-9/pdf>
- Wilson, C. M., Johansson, G., Pourkabirian, A., Simoen, M., Johansson, J. R., Duty, T., ... & Delsing, P. (2011). Observation of the dynamical Casimir effect in a superconducting circuit. *Nature*, 479(7373), 376–379. <https://www.nature.com/articles/nature10561.pdf>
- Yang, Y., & Kawazoe, Y. (2012). Characterization of zero-point vibration in one-component crystals. *EPL (Europhysics Letters)*, 98(6), 66007. <https://iopscience.iop.org/article/10.1209/0295-5075/98/66007/pdf>

APPENDIX I: CALCULATION OF CURRENT AND POWER AVAILABLE FROM THE QUANTUM VACUUM

The available current and power from the background quantum vacuum electromagnetic radiation is derived here. I start with the energy density of electromagnetic modes in space, $\rho(hf)$, given in Equation (1). Although the vacuum state has only virtual photons (Milonni, 2013), a naive calculation of the flux density of ZPE photons striking a surface can be carried out as follows. The flux is equal to the energy density divided by the photon energy,

hf , times the velocity of photons, c . Just as with the usual Stefan Boltzmann law for blackbody radiation, a geometric factor of $\frac{1}{4}$ must be included. The photon flux per unit frequency is then:

$$j = \rho(hf) \frac{c}{4hf} \quad (2)$$

To find the total flux available over a range of frequencies, the expression for $\rho(hf)$ from Equation (1) is inserted into Equation (2), and the flux is integrated up to a cutoff frequency, f_{co} . Keeping only the righthand bracketed ZPE term in Equation (1), $hf/2$, the total flux is:

$$\Delta J = \frac{\pi}{c^2} \int_0^{f_{co}} f^2 df = \frac{\pi}{3h^3 c^2} (hf_{co})^3 \quad (3)$$

This cumulative photon flux is substantial. For example, with a cutoff energy of 4 eV it is 1028 photons $\text{m}^{-2} \text{s}^{-1}$, corresponding to a photon current of 1.7 GA m^{-2} , where photon current is defined as the electrical current that would be produced if each incident photon generated the current from one electron.

To find the cumulative power available, the photon current at each energy in the integral in Equation (3) is multiplied by the photon energy:

$$P = \frac{\pi}{c^2} \int_0^{f_{co}} hf^3 df = \frac{\pi}{4h^3 c^2} (hf_{co})^4 \quad (4)$$

For the same 4 eV cutoff, the available power is 5.0 GW m^{-2} .

APPENDIX II: TESTS FOR ARTIFACTS

An extensive discussion of much of the investigation of artifacts is presented by Model et al. (2021a), except where noted with other references below.

One question is whether the results we see are just a short-term effect due to charging of interfaces or chemical reactions. To test for that, we continuously measured the current output over 4 hours, and later over 24 hours, to see if it declined. For example, if there were one charge trapped at each insulator molecule, they could produce the observed current for 3 μs . We found no change in the output, even over 24 hours. What we observe is not a transient effect.

If what we observe is due to harvesting of current over the active area of the device, as opposed to energy coming from another part of the circuit, the current should scale with device area. We found that the current scaled with area for areas extending from 6 to 10,000 μm^2 . Similarly, the output should scale with number of devices in an array. We found that two different types of 4 x 4 arrays produce 4 times the current and 4 times the voltage of individual devices, showing the expected scaling.

Another question is whether the output is genuinely due to the adjoining optical cavity or might be the result of the way the MIM structure was processed after it was formed in order to produce the adjoining cavity. We measured devices at three different stages in the fabrication up through the deposition of the transparent dielectric in the cavity and found no output current; only when we deposited the final mirror layer did the power production appear. The output is not due to a quirk in the processing, but is instead produced only in the completed device.

There are several ways that the observed power output might inadvertently be due to pickup of charge or electromagnetic fields:

- To determine whether the current might be due to charge on the mirror that leaked through to the MIM structure, we compared the resistance of the optical cavity to that of the MIM device. For each optical cavity thickness we found that the cavity resistance was a least one million times higher than that of the MIM structure, so that any charge that inadvertently formed on the mirror could not leak through to the MIM region, through which the current is measured (see Figure 3(a)).
- Recently, we checked whether a voltage applied to the mirror might somehow create a field effect that induced current through the MIM structure. For mirror voltages up to 10 V, we found no effect on the MIM current (Weerakkody, unpublished 2022).
- To check for electromagnetic pickup we measured the $I(V)$ characteristics of a device in a mu-metal box, which blocks low frequencies, and in an aluminum box, which blocks higher frequencies, and found no change from devices measured in ambient conditions.

Thermoelectric voltages, i.e., voltages due to temperature differences in locations on a device or in a measurement system, plague low-power measurements. Three different tests were carried out to test for possible thermoelectric voltages between the device and the measurement system:

- To compensate for such voltages, most measurements were carried out using a voltage reversal method as follows: two measurements were carried out with currents of opposite polarity, i.e., one when the base electrode was grounded and another when the upper electrode was grounded, and then the difference in the currents was subtracted to yield the final value.
- The fact that the 4 x 4 arrays discussed above yield four times the voltage output of a single device indicates that this voltage is not due to thermoelectric voltages between the device and the measure-

ment system, which would not scale with number of devices in series.

- Recently preliminary measurements were carried out as the device temperature was reduced from approximately room temperature (300 K) to approximately 80 K, and only small changes, within experimental error, were observed in the device output (Weerakkody, unpublished 2022).

To test whether the results could be due to temperature gradients within the sample, we carried out two tests:

- The temperature difference between the environment above the devices and the measurement stage was varied, and no change in the output was observed.

- Devices were measured inside a closed cryostat at a rigorously maintained uniform temperature, and the output was unchanged (Weerakkody, unpublished 2022).

For the reasons given, it appears unlikely that any thermoelectric effect is producing the results that we observe.

Calculations of the expected current resulting from absorption of known fluxes of cosmic rays and of solar neutrinos could not produce the currents that we observed.

In summary, we have examined all the potential artifacts that we and outside critics have suggested might be the source for the observed power production from our devices, and none can explain the results.